An Experimental Investigation of the Shape Deviation of SLM Printed Parts

Thai Son Nguyen
Center for Transport Science and Technology, University of Transport and Communications, Hanoi, Vietnam | National Research Institute of Mechanical Engineering, Hanoi, Vietnam
sonnt2@utc.edu.vn

Ngoc Hien Tran
Faculty of Mechanical Engineering, University of Transport and Communications, Hanoi, Vietnam
tranhien.tkm@utc.edu.vn (corresponding author)

Received: 16 June 2025 | Revised: 10 July 2025 | Accepted: 23 July 2025

 DOI: https://doi.org/10.48084/etasr.12777

ABSTRACT

The 3D printing technology is increasingly used in manufacturing, medicine, education, and various other fields. This technology allows for the creation of parts with complex shapes, which would be difficult or even impossible to manufacture using traditional machining methods. However, the quality of the printed products is still a barrier to the widespread use of the 3D printing technology in industrial applications. The former includes the accuracy of the shape, size, and mechanical properties of the printed products. Research to improve the efficiency of the printing process and the printed product quality is essential for application fields. This study, through experiments, determines the relationship between the shape deviation of the printed products and the set of printing parameters. The latter includes the laser power, printing speed, and printing layer thickness. Experimental studies were conducted on the FF-M180D printer using the Selective Laser Melting (SLM) printing method. Ti6Al4V powder is utilized as printing material for this study. Based on the regression model showing the relationship between the printing parameters and shape deviation, the optimal set of parameters to minimize the shape deviation was determined.

Keywords-Selective Laser Melting (SLM); optimal printing parameters; shape deviation; regression model; quality of printed products

I. INTRODUCTION

3D printing or additive manufacturing is a method of creating 3D products by adding material layer by layer, allowing the creation of products with complex shapes. Since the 1980s, the 3D printing technology has been proposed for application in the product design stage, using plastic materials. Nowadays, with the advancement of science, technology, and new materials, many printing methods are employed for plastics and other materials, such as metals and composites [1]. On the other hand, the 3D printing technology is not only used in the design stage to create the initial prototypes, but is also utilized to create the final products [2]. This means that the created products ensure the geometric accuracy while satisfying the mechanical and physical criteria to meet the requirements of the final product. According to ASTM standards, the additive manufacturing technology is classified into 7 groups: powder bed fusion, directed energy deposition, binder jetting, material jetting, material extrusion, vat photopolymerization, and sheet lamination, as shown in Figure 1 [3].

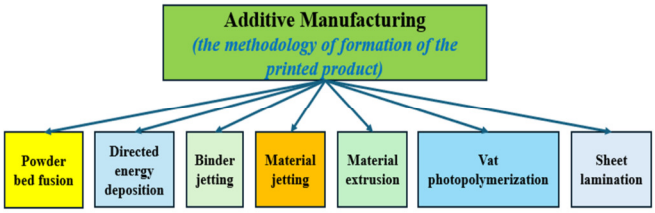

Fig. 1. Classification of additive manufacturing.

There are various printing methods in the powder bed fusion group, namely the Selective Laser Sintering (SLS), Hot Isostatic Pressing (HIP), Direct Metal Sintering (DMLS), laser micro sintering, SLM, and laserCUSING process [4]. Among these methods, SLM is commonly used to print parts from metal powder. The principle of 3D printing deploying the SLM method is depicted in Figure 2. In the SLM method, with the first printed layer, the powder layer is spread on a substrate. After the powder is spread, the laser source changes the sintering position through the optical system to sinter the powder layer. Once the first layer is printed, the machine table is lowered vertically by an amount equal to the thickness of the printed layer. The powder feeding system spreads a layer of

powder on the newly printed layer. Then, this layer of powder is sintered by the laser source. This process is repeated until the full height of the 3D model is printed. After printing, the product is often post-processed to relieve the residual stress caused by the rapid cooling through the annealing method. The final product is then cut from the substrate employing a method known as Electrical Discharge Machining (EDM).

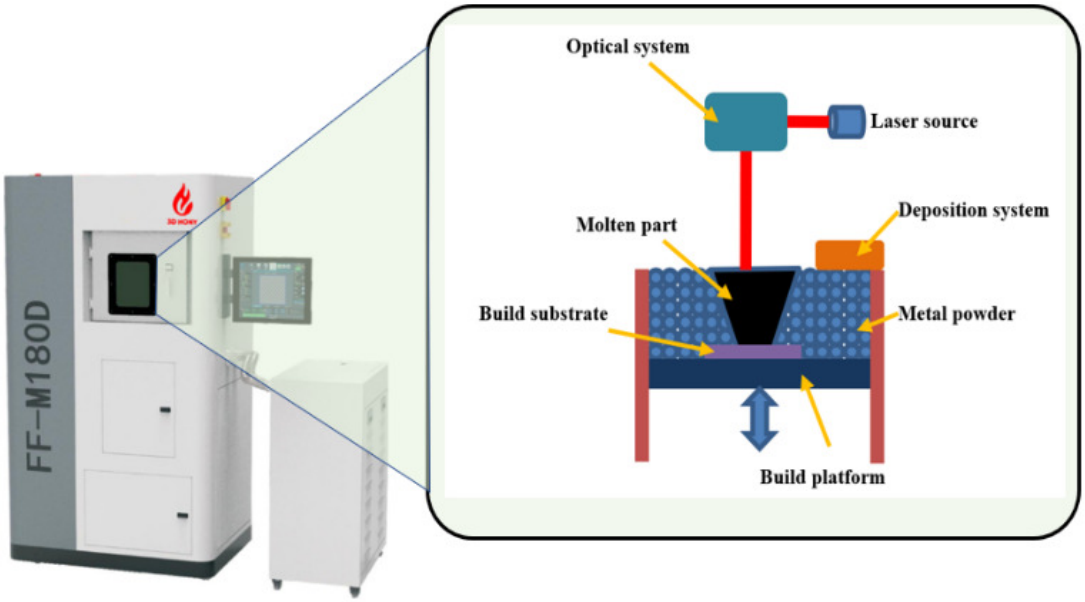

Fig. 2. FF-M180D machine and mechanism of SLM.

High-quality printed products exhibit geometric shape accuracy, dimensional accuracy, and mechanical and physical properties that ensure the working requirements of the product [5, 6]. Most studies focus on the surface quality and mechanical properties, while the shape accuracy, one of the most important criteria affecting the product quality, especially that of the final product, is less studied [7, 8]. The shape deviation includes the positive deviation and the negative deviation, which represent the difference between the desired part shape and the obtained part shape, as shown in Figure 3.

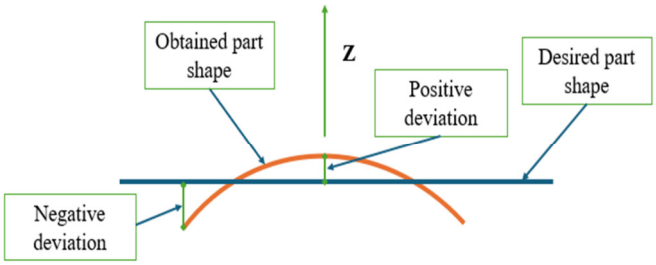

Fig. 3. Definition of the shape deviation.

The shape deviation in the printed product arises due to the effect of the thermal energy during the sintering process of the metal powder and the rapid phase transition between the solid and liquid states. Authors in [7] conducted experimental studies on the influence of printing parameters, including laser power and printing speed, on the shape accuracy when printing AlSi10Mg alloy powder using the SLM method. In this experimental study, the laser power was varied in the range of 170 W-390 W, the printing speed ranged from 534 mm/s to 1225 mm/s, and the printing layer thickness was kept constant at 0.03 mm. The change in printing layer thickness is also an important factor affecting the accuracy of the printed products, but it was not considered in this study. In addition to the printing parameters, design parameters, such as part orientation, part thickness, build position, and feature size also influence the geometric accuracy of the printed parts [9].

Authors in [10] carried out an experimental research for determining the shape deviation for the parts printed by additive manufacturing. In this research, the layer thickness was considered. However, the printed material is plastic with the fused deposition modeling printing method being utilized. Authors in [11] studied the shape deviation of horizontal interior circular channels fabricated by laser powder bed fusion with the 316L stainless steel powder. With the laser power ranging from 60 W to 100 W and the printing speed ranging from 150 mm/s to 350 mm/s, it was shown that the shape deviation decreased with decreasing the laser power and increasing the printing speed. Authors in [12] carried out experiments for samples printed employing the SLM method using an AlSi10Mg alloy. The SLM machine with 200 W laser power and 250 mm/s printing speed for printing holes was used, and then a FARO Quantum V2 FaroArm 3D scanner was utilized for measuring the shape deviation. The experimental results demonstrated that the largest dimensional deviation was 0.423 mm corresponding to a hole with a diameter of 6 mm. Authors in [13] conducted a simulation and experimental research on the SLM printing process with 17-4 PH steel

material, laser power 183 W, and printing speed 1045 mm/s and found that the size deviation is not greater than 10%. Authors in [14] carried out an experimental study on the SLM printing with Ti6Al4V powder in which the laser power parameters varied from 55 W to 95 W, the printing speed from 150 mm/s to 1000 mm/s, and the line spacing from 0.0495 mm to 0.099 mm. The maximum dimensional deviation was + 2.09 mm. The best dimensional accuracy was achieved with the highest printing speed and medium laser power.

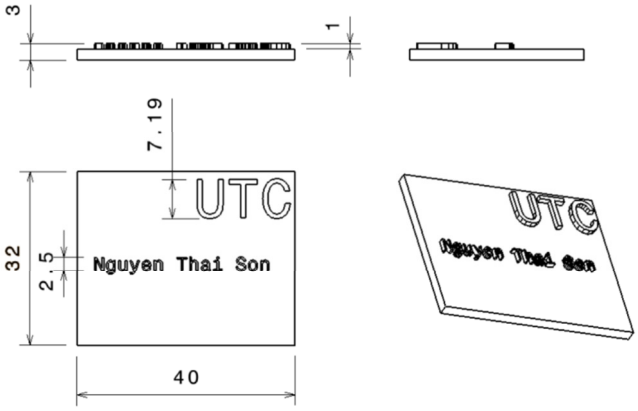

Fig. 4. Shape and size of the printed sample.

The quality of the 3D printed products depends on four groups of factors, including the printing method, printer accuracy, printing process parameters, and printing materials [15]. In this study, through experiments performed using the SLM method and Ti6Al4V powder material, the relationship between the geometric shape accuracy and printing parameters was established. Deploying a regression model to demonstrate this relationship, a set of printing process parameters was determined to ensure the smallest shape deviation.

II. MATERIAL AND EXPERIMENTS

Ti6Al4V titanium alloy powder material with a large particle size distribution ranging from 25 µm to 63 µm was used to print the samples. The percentage distribution of the particle diameter (d) is: $d \leq 25$ µm, accounting for 0.8%; d in the range of 25 µm to 63 µm, accounting for 83.4%; and $d > 63$ µm, accounting for 15.8%. The shape and size of the printed samples are shown in Figure 4. The dimensions of the sample (length × width × height) are 40 mm × 32 mm × 3 mm, respectively. The FF-M180D printer using the SLM printing method was utilized to print the samples. The printer's technical parameters are: 1000 W laser source; maximum print size with a diameter of 180 mm; print height of 100 mm; and print layer depth from 0.02 mm to 0.06 mm. The protective gas in the printing chamber is Argon. The objective of the experimental study is to establish a mathematical model that shows the relationship between the geometric deviation and printing process parameters. Then, the optimal printing process parameters are determined to minimize the geometric deviation. Figure 5 displays the systematic procedure for carrying out the experiments. The steps include: determining the printing parameters; printing the samples; determining the shape deviation; and establishing the regression model.

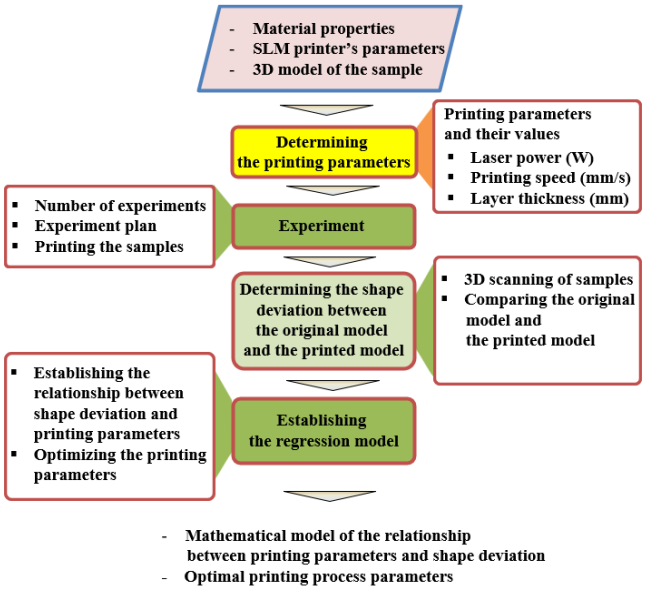

Fig. 5. Systematic procedure for carrying out the experiments.

The input parameters, such as the printer specifications and material properties, are crucial for determining the appropriate range of the printing process parameters. For the materials, the printing temperature must reach the phase transition point from solid to liquid. If the temperature is not enough, sintering will not occur; if the temperature is too high, the material will change from liquid to vapor. Therefore, it is necessary to accurately determine the phase transition temperature of the material. For the Ti6Al4V material, the melting temperature is 1877 K [16]. During the printing process, the printing temperature depends on the set of printing process parameters including the laser power, printing speed, and printing layer thickness [17]. Regarding the printing temperature, whether it is high or low, largely depends on the laser power. On the other hand, changing the values of the printing parameters will affect the volumetric energy density (E), which is calculated as [18]:

$$E = \frac{U}{V.t.h.} (\text{J/mm}^3) \quad (1)$$

where U is laser power (W), V is the printing speed (mm/s). h is the hatching distance (mm), and t is the layer thickness (mm).

A higher value of E results in a lower porosity and an improved quality of the printed product [19]. However, the appropriate value of the volumetric energy density (E) depends on the material properties and printing process parameters. For the Ti6Al4V material, research suggests different E values based on the desired porosity, microstructure, and mechanical properties of the printed product, such as E values ranging from 24.2 J/mm^3 to 71.4 J/mm$_3$ [20]; $E >$ 70 J/mm^3 [21]; and E = 184 J/mm^3 [22]. To determine the range of the printing process parameters, a simulation study using COMSOL software was conducted [23, 24], and initial experiments were also performed using the FF-M180D printer.

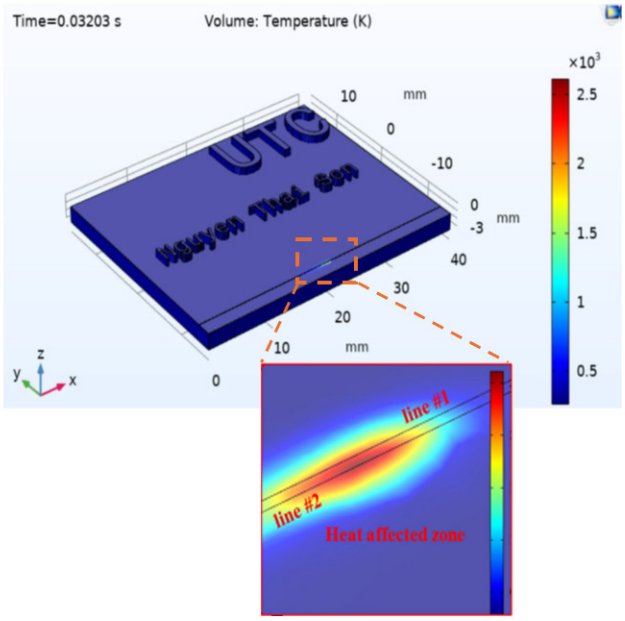

Fig. 6. Temperature distribution during the printing process.

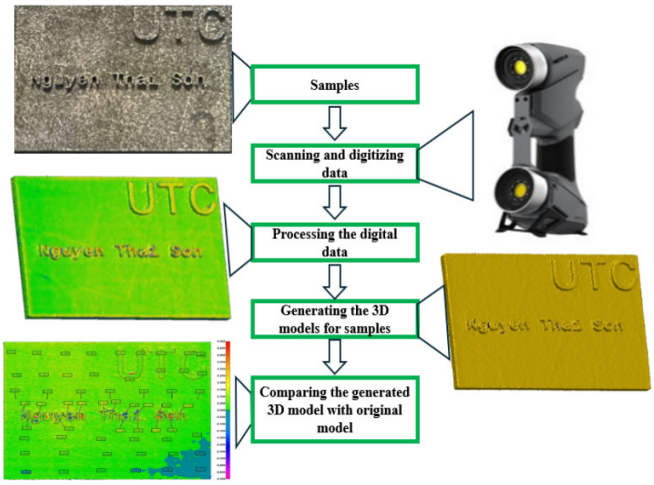

Fig. 7. Steps for determining the shape deviation.

Figure 6 illustrates the temperature distribution during printing. With the values of the printing process parameters, including laser power 300 W, printing speed 1000 mm/s, and layer thickness 0.03 mm, the temperature achieved during printing is 2500 K. The hatch distance, which was kept constant with the samples, is 140 μm. These printing process parameters ensure the sintering of the material during printing. From the results of the simulation and initial experiments, the ranges of the printing process parameters used in the experiment are:

- 150 ≤ Laser power ≤ 350 (W)
- 400 ≤ Printing speed ≤ 1500 (mm/s)
- 0.03 ≤ Layer thickness ≤ 0.06 (mm)

Employing the three input factors of the printing process mentioned above, a full two-level factorial experiment requires 8 runs. This design is improved by adding one center point [25]. The center point appears at the ninth row in Table I. The steps followed to determine the shape deviation of the printed samples from the requirements are shown in Figure 7. These steps include scanning and digitizing the data from the samples, processing the digital data, generating the 3D models for the samples using the Geomagic Wrap software [26], and comparing the gendered 3D model with the original model. To create the 3D models of the printed samples, the HandySCAN 3D machine with a non-contact 3D scanning method is deployed. The printed samples were scanned, and the scan data, which were initially a point cloud, were processed into a solid model. This model is compared with the original model of the printed sample to determine the shape deviation.

TABLE I. EXPERIMENT DESIGN

Samples	Laser power (W)	Printing speed (mm/s)	Layer thickness (mm)	Geometric deviation (mm)
1	150	400	0.030	0.319
2	350	400	0.030	0.611
3	150	1500	0.030	0.142
4	350	1500	0.030	0.121
5	150	400	0.060	0.682
6	350	400	0.060	0.664
7	150	1500	0.060	0.447
8	350	1500	0.060	0.370
9	250	950	0.045	0.417

III. RESULTS AND DISCUSSION

Nine printed samples were measured and compared with the original model. The shape deviations are represented using different colors: green indicates no deviation, red indicates a positive deviation, and blue indicates a negative deviation. The measurement results for the largest shape deviations in the nine printed samples are presented in Table I. Among the printed samples, sample number 4 has the smallest shape deviation corresponding to the laser source U = 350 W, printing speed V = 1500 mm/s, and layer thickness t = 0.03 mm, as portrayed in Figure 8. Sample number 5 has the largest shape deviation corresponding to the laser source U = 150 W, printing speed V = 400 mm/s, and layer thickness t = 0.06 mm, as illustrated in Figure 9. Minitab software was used to determine the regression model using experimental data [27]. The regression model demonstrates the relationship between the shape deviation (D) and the printing process parameters, including the laser power (U), printing speed (V), and layer thickness (t):

$$D = -0.6071 + 0.004041\,U + 0.000278\,V + 22.862\,t - 0.000003\,UV - 0.06706\,Ut - 0.007530\,Vt + 0.000038\,UVt \text{ (mm)} \quad (2)$$

The variables U, V, and t, along with their interactions UV, Ut, Vt, and UVt are all significant in the regression model with the P-value being less than 0.05, as evidenced in Table II. Also, from the Pareto chart in Figure 10, it can be seen that the variables and their interactions affect the objective function (D) in which the printing speed has the greatest influence on the shape deviation of the printed part.

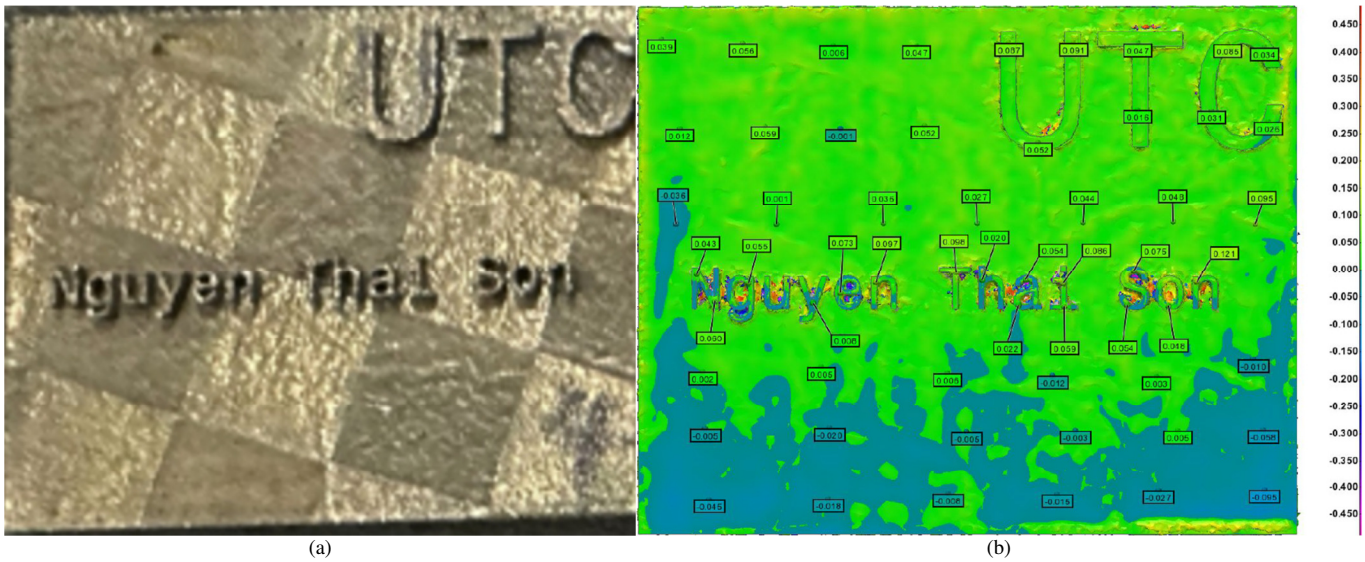

(a) (b)

Fig. 8. Sample number 4 with the smallest shape deviation.

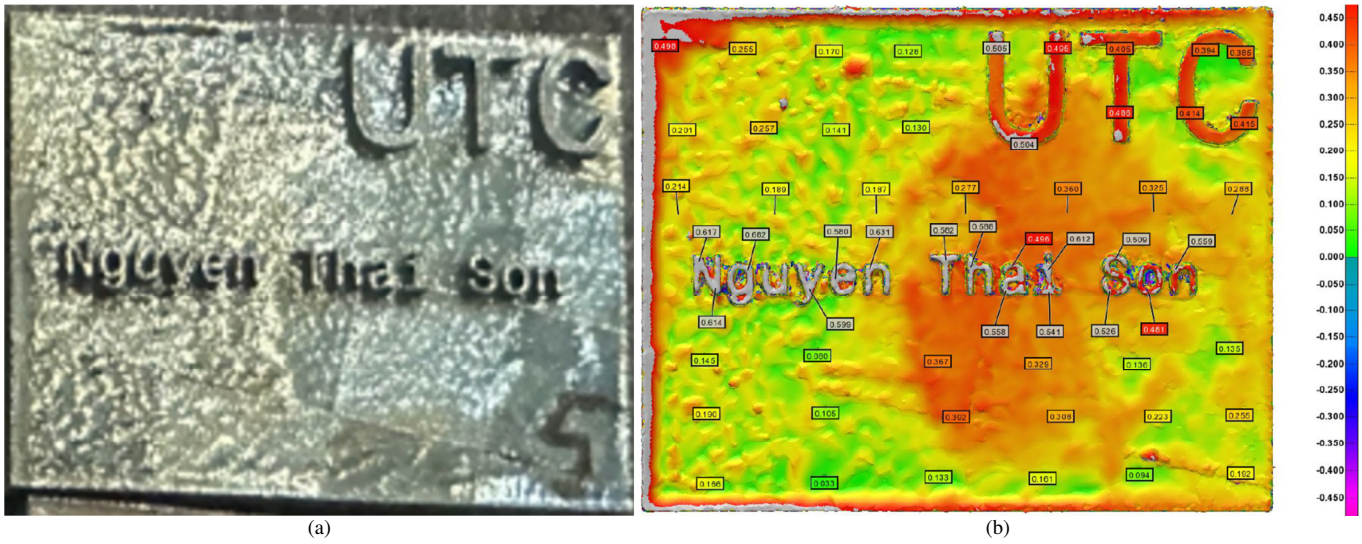

(a) (b)

Fig. 9. Sample number 5 with the largest shape deviation.

TABLE II. VARIABLES ANALYSIS

Term	Coefficient	P-value
U	0.004041	0.024
V	0.000278	0.004
t	22.86200	0.004
UV	-0.000003	0.011
Ut	-0.067060	0.012
Vt	-0.007530	0.031
UVt	0.000038	0.017

Equation (2) is used to determine the shape deviation in relation to three printing parameters, namely the laser power, printing speed, and layer thickness. The shape deviation when printing holes using the EP-M100T printer with 316L steel powder is evaluated in relation to two printing parameters: the laser power and printing speed [11].

The layer thickness is another important factor affecting the shape accuracy. The larger the layer thickness is, the more the shape deviation increases, as illustrated in Figures 11-14. Based on the regression model established in (2), the relationship between D and the variables U, V, and t was analyzed to determine the optimal printing process parameters. This analysis is exhibited in Figures 11-14, corresponding to t values of 0.03, 0.04, 0.05, and 0.06 mm, respectively. Based on the results, some conclusions drawn regarding the values of the printing process parameters are:

- The smallest shape deviation is achieved at higher printing speeds and at a lower layer thickness. When compared with the findings in [14] using the Ti6Al4V material, the shape deviation decreased when the printing speed increased.
- With the Ti6Al4V powder printed on the SLM printer, the shape deviation decreased with an increase in the printing speed, and the average laser power range was 150 W to 350 W. This result is consistent with the findings of [11].

- With a layer thickness t = 0.03 mm, the shape deviation was less than 0.2 mm, which is within the acceptable limit for the printing speed range of 1250 mm/s-1500 mm/s and the laser power range of 150 W-350 W, as presented in Figure 11.

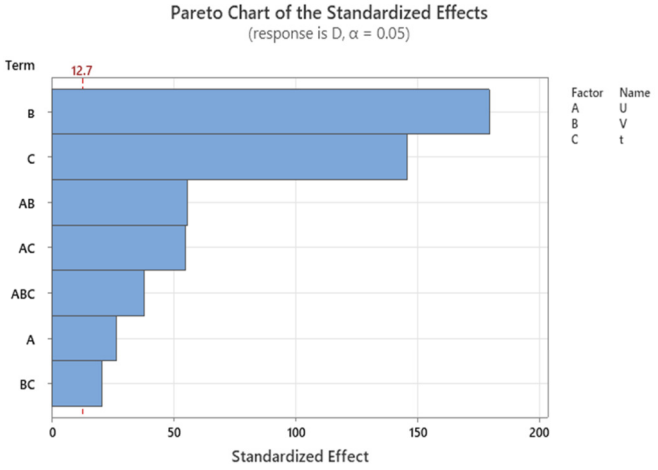

Fig. 10. Pareto chart of variables.

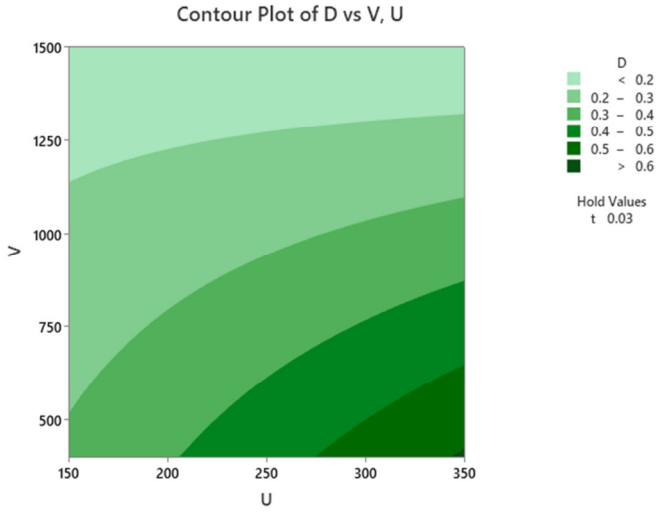

Fig. 11. Relationship between shape deviation (D), laser power (U), and printing speed (V) at t = 0.03 mm.

- To achieve a shape deviation of less than 0.3 mm at t = 0.05 mm, as shown in Figure 13 and t = 0.06 mm, as portrayed in Figure 14, high values of laser power (U) and printing speed (V) are required.
- In this study, the largest shape deviation (D) was 0.682 mm, corresponding to a laser power of 150 W, printing speed of 400 mm/s, and printing layer thickness of 0.06 mm.
- The optimal printing parameters were achieved with t = 0.03 mm, U = 350 W, and V = 1500 mm/s, corresponding to D = 0.1207 mm.

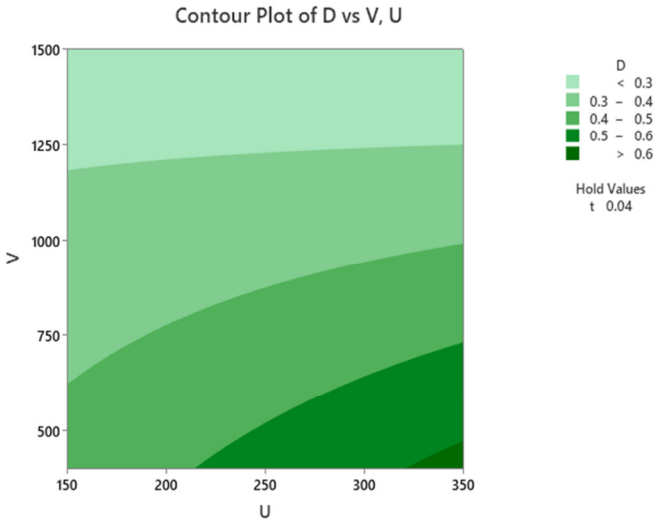

Fig. 12. Relationship between D with U, V when t = 0.04 mm.

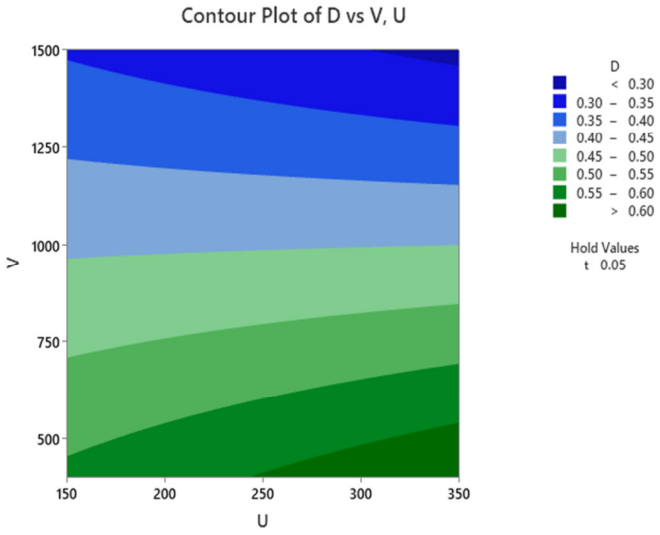

Fig. 13. Relationship between shape deviation (D), laser power (U), and printing speed (V) at t = 0.05 mm.

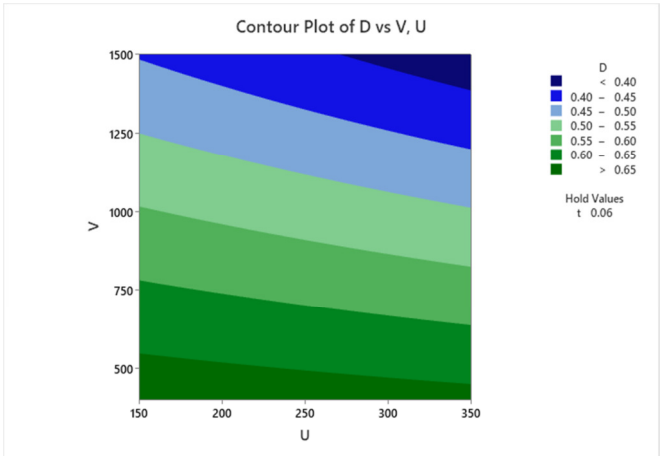

Fig. 14. Relationship between shape deviation (D), laser power (U), and printing speed (V) at t = 0.06 mm.

IV. CONCLUSIONS

The printed product quality is always a concern in the additive manufacturing process. The former is assessed through the criteria of geometric accuracy, dimensional accuracy, and mechanical and physical property requirements. There are many factors affecting the printing quality, among which the printing parameters have a significant influence. In this study, the relationship between the printing process parameters, including the laser power, printing speed, and layer thickness, with the shape deviation of the printed product has been established. This relationship was expressed using a regression model. Based on this model, the influence of the printing process parameters on the objective function was analyzed to determine the optimal process parameters.

The temperature during printing plays an important role in the quality of the printing process. The printing parameters must ensure that the generated temperature is higher than the melting temperature (*Tm*) and lower than the boiling temperature of the material. If the generated temperature is less than the *Tm*, the material does not melt, and if the generated temperature is much higher than the *Tm*, it adversely affects the printing quality and the efficiency of the printer. This study contributes towards establishing optimum printing parameters, including laser power, printing speed, and layer thickness, for the Ti6Al4V powder material using the Selective Laser Melting (SLM) printing method, to ensure an effective printing temperature.

Future studies could explore the influence of the printing process parameters on the internal structure and surface quality, and the influence of these factors on the mechanical and physical properties of the printed product.

ACKNOWLEDGMENT

This research was funded by Vietnam Ministry of Education and Training, grant number: B2025-GHA-06.

REFERENCES

[1] S. Park, W. Shou, L. Makatura, W. Matusik, and K. (Kelvin) Fu, "3D printing of polymer composites: Materials, processes, and applications," *Matter*, vol. 5, no. 1, pp. 43–76, Jan. 2022, https://doi.org/10.1016/j.matt.2021.10.018.

[2] R. Kumar, M. Kumar, and J. S. Chohan, "The role of additive manufacturing for biomedical applications: A critical review," *Journal of Manufacturing Processes*, vol. 64, pp. 828–850, Apr. 2021, https://doi.org/10.1016/j.jmapro.2021.02.022.

[3] I. Yadroitsev, I. Yadroitsava, A.D. Plessis, "Basics of laser powder bed fusion," in *Fundamentals of Laser Powder Bed Fusion of Metals*, Elsevier, 2021, pp. 15–38.

[4] N.S. Moghaddam, A. Jahadakbar, A. Amerinatanzi, and M. Elahinia, "Recent Advances in Laser-Based Additive Manufacturing," in *Laser-Based Additive Manufacturing of Metal Parts*, 1st ed., Boca Raton: CRC Press, Taylor & Francis, 2018.: CRC Press, 2017, pp. 1–24.

[5] A. Karadag and O. Ulkir, "Prediction of Dimensional Accuracy and Surface Quality in Additively Manufactured Biomedical Implants Using ANN," *International Journal of Precision Engineering and Manufacturing*, vol. 26, no. 5, pp. 1187–1213, May 2025, https://doi.org/10.1007/s12541-025-01229-2.

[6] S. Rouf, A. Raina, M. Irfan Ul Haq, N. Naveed, S. Jeganmohan, and A. Farzana Kichloo, "3D printed parts and mechanical properties: Influencing parameters, sustainability aspects, global market scenario, challenges and applications," *Advanced Industrial and Engineering Polymer Research*, vol. 5, no. 3, pp. 143–158, Jul. 2022, https://doi.org/10.1016/j.aiepr.2022.02.001.

[7] Y. Siyambaş and Y. Turgut, "Experimental investigation and optimization of the effects of manufacturing parameters on geometric tolerances in additive manufacturing of AlSi10Mg alloy," *The International Journal of Advanced Manufacturing Technology*, vol. 134, no. 1–2, pp. 415–429, Sep. 2024, https://doi.org/10.1007/s00170-024-14128-z.

[8] R. Sheshadri *et al.*, "Experimental investigation of selective laser melting parameters for higher surface quality and microhardness properties: taguchi and super ranking concept approaches," *Journal of Materials Research and Technology*, vol. 14, pp. 2586–2600, Sep. 2021, https://doi.org/10.1016/j.jmrt.2021.07.144.

[9] R. Biswal and A. Ganesan, "Experimental investigation of design parameters on geometrical accuracy of selective laser sintered parts," *Journal of Manufacturing Processes*, vol. 108, pp. 48–61, Dec. 2023, https://doi.org/10.1016/j.jmapro.2023.10.059.

[10] A. D. Rizea, D. C. Anghel, and D. M. Iordache, "Study of the deviation of shape for the parts obtained by additive manufacturing," *IOP Conference Series: Materials Science and Engineering*, vol. 1009, no. 1, Jan. 2021, Art. no. 012050, https://doi.org/10.1088/1757-899x/1009/1/012050.

[11] S. Feng, S. Chen, A. M. Kamat, R. Zhang, M. Huang, and L. Hu, "Investigation on shape deviation of horizontal interior circular channels fabricated by laser powder bed fusion," *Additive Manufacturing*, vol. 36, Dec. 2020, Art. no. 101585, https://doi.org/10.1016/j.addma.2020.101585.

[12] R. Madaj, R. Kohar, F. Brumercik, and M. Veres, "Design Study of Hole Types for Improved Cooling of Experimental Heatsinks Manufactured by SLM Technology Using an AlSi10Mg Alloy," *Applied Sciences*, vol. 15, no. 4, Feb. 2025, Art. no. 2118, https://doi.org/10.3390/app15042118.

[13] D. Bompos, J. Chaves-Jacob, and J.-M. Sprauel, "Shape distortion prediction in complex 3D parts induced during the selective laser melting process," *CIRP Annals*, vol. 69, no. 1, pp. 517–520, 2020, https://doi.org/10.1016/j.cirp.2020.04.014.

[14] S. Pal *et al.*, "Dimensional deviations in Ti-6Al-4V discs produced with different process parameters during selective laser melting," *The International Journal of Advanced Manufacturing Technology*, vol. 129, no. 11–12, pp. 5655–5669, Dec. 2023, https://doi.org/10.1007/s00170-023-12620-6.

[15] C. Herpel *et al.*, "Accuracy of 3D printing compared with milling — A multi-center analysis of try-in dentures," *Journal of Dentistry*, vol. 110, Jul. 2021, Art. no. 103681, https://doi.org/10.1016/j.jdent.2021.103681.

[16] J. J. Z. Li, W. L. Johnson, and W.-K. Rhim, "Thermal expansion of liquid Ti–6Al–4V measured by electrostatic levitation," *Applied Physics Letters*, vol. 89, no. 11, Sep. 2006, https://doi.org/10.1063/1.2349840.

[17] V. E. Alexopoulou, E. L. Papazoglou, P. Karmiris-Obratański, and A. P. Markopoulos, "3D finite element modeling of selective laser melting for conduction, transition and keyhole modes," *Journal of Manufacturing Processes*, vol. 75, pp. 877–894, Mar. 2022, https://doi.org/10.1016/j.jmapro.2022.01.054.

[18] R. Zhao *et al.*, "On the role of volumetric energy density in the microstructure and mechanical properties of laser powder bed fusion Ti-6Al-4V alloy," *Additive Manufacturing*, vol. 51, Mar. 2022, Art. no. 102605, https://doi.org/10.1016/j.addma.2022.102605.

[19] A. Leicht, M. Fischer, U. Klement, L. Nyborg, and E. Hryha, "Increasing the Productivity of Laser Powder Bed Fusion for Stainless Steel 316L through Increased Layer Thickness," *Journal of Materials Engineering and Performance*, vol. 30, no. 1, pp. 575–584, Jan. 2021, https://doi.org/10.1007/s11665-020-05334-3.

[20] C. M. Cepeda-Jiménez, F. Potenza, E. Magalini, V. Luchin, A. Molinari, and M. T. Pérez-Prado, "Effect of energy density on the microstructure and texture evolution of Ti-6Al-4V manufactured by laser powder bed fusion," *Materials Characterization*, vol. 163, May 2020, Art. no. 110238, https://doi.org/10.1016/j.matchar.2020.110238.

[21] A. Zafari, M. R. Barati, and K. Xia, "Controlling martensitic decomposition during selective laser melting to achieve best ductility in high strength Ti-6Al-4V," *Materials Science and Engineering: A*, vol.

744, pp. 445–455, Jan. 2019, https://doi.org/10.1016/j.msea.2018.12.047.

[22] M. Sangali, A. Cremasco, J. Soyama, R. Caram, and R. J. Contieri, "Selective Laser Melting of Ti-6Al-4V Alloy: Correlation Between Processing Parameters, Microstructure and Corrosion Properties," *Materials Research*, vol. 26, no. suppl 1, 2023, https://doi.org/10.1590/1980-5373-mr-2023-0055.

[23] H. S. Park, N. H. Tran, V. T. Hoang, and V. H. Bui, "Development of a Prediction System for 3D Printed Part Deformation," *Engineering, Technology & Applied Science Research*, vol. 12, no. 6, pp. 9450–9457, Dec. 2022, https://doi.org/10.48084/etasr.5257.

[24] *COMSOL Multiphysics*. COMSOL Multiphysics Pvt. Ltd, Accessed: 15 Mar. 2025, [Online]. Available: https://www.comsol.com/products.

[25] G. W. Oehlert, *A first course in design and analysis of experiments*, 1st ed. New York: W.H. Freeman, 2000.

[26] *Geomagic wrap*. Hexagon, Accessed: 7 April 2025. [Online]. Available: https://hexagon.com/products/geomagic-wrap.

[27] *Minitab*. Minitab LLC, Accessed: May 12, 2025. [Online]. Available: https://www.minitab.com/en-us/.

AUTHORS PROFILE

Thai-Son Nguyen received the B.Sc. degree from the University of Rennes 1 and the M.Sc. degree in Mechatronic from the University of Rennes 1 in France, in 2016 and 2019, respectively. Currently, he is a PhD candidate in Mechanical Engineering at the National Research Institute of Mechanical Engineering and works at the Center for Transport Science and Technology, University of Transport and Communications, Vietnam. His research interests include CAD/CAM/CNC and additive manufacturing.

Ngoc-Hien Tran received the B.Sc. degree from the University of Transport and Communications and the M.Sc. degree in Mechanical Engineering from Hanoi University of Technology, in 2001 and 2007, respectively, in Vietnam. He received his Ph.D. degree in Mechanical Engineering from Ulsan University in Korea in 2011. Currently, he is an associate professor at the Faculty of Mechanical Engineering, University of Transport and Communications, Hanoi, Vietnam. His research interests include CAD/CAM/CAE, Intelligent Manufacturing System, and Additive Manufacturing. His researches are published in some ISI Journals, and Conference Proceedings.